Intracellular Axial Current in *Chara corallina* Reflects the Altered Kinetics of Ions in Cytoplasm under the Influence of Light

F. Baudenbacher,* L. E. Fong,* G. Thiel,† M. Wacke,† V. Jazbinsek,‡ J. R. Holzer,* A. Stampfl,‡ and Z. Trontelj‡
*Department of Physics and Astronomy, Vanderbilt University, Nashville, Tennessee 37235; †Institute for Botany, Plant Biophysics, Darmstadt University of Technology, D-64287 Darmstadt, Germany; and ‡Physics Department, Institute of Mathematics, Physics and Mechanics, University of Ljubljana, 1000 Ljubljana, Slovenia

ABSTRACT Recent experiments demonstrate that the concentration of Ca^{2+} in cytoplasm of *Chara corallina* internodal cells plays important role in electrical excitation of the plasma membrane. The concentration of free Ca^{2+} in the cytoplasm $-[Ca^{2+}]_c$ is also sensitive to visible light. Both phenomena were simultaneously studied by noninvasive measuring action potential (AP) and magnetic field with a superconducting quantum interference device magnetometer in very close vicinity of electrically excited internodal *C. corallina* cells. A temporal shift in the depolarization maximum, which progressively occurred after transferring cells from the dark into the light, can be explained by the extended Othmer model. Assuming that the change in membrane voltage during the depolarization part of AP is the direct consequence of an activation of $[Ca^{2+}]_c$ sensitive Cl^- channels, the model simulations compare well with the experimental data. We can say that we have an example of electrically elicited AP that is of biochemical nature. Electric and magnetic measurements are in good agreement.

INTRODUCTION

The green algae from the family of the *Characeae* have a long history as a model system for ion transport in plants (Umrath, 1929; Hope and Findlay, 1964; Hope and Walker, 1975; Tazawa et al., 1987). Experimental work was favorable given the very large geometry of a single internodal cell and the many possibilities of manipulating these cells with microsurgery (Shimmen et al., 1994; Beilby, 1990). In this sense, the species *Chara corallina* is the plant equivalent to the squid axon in the study of ion transport in plants.

The recent phylogenetic analysis of the *Characeae* has again strengthened the model character of *Chara*. This family of green algae is now seen as the ancestor of higher plants (Kranz et al., 1995; Karol et al., 2001). Hence, an investigation of the physiological processes in *Chara* is interesting from an evolutionary point of view. Also, data from the simple single-cell system can be seen as a common primitive mechanism for comparable effects in higher plants.

The plasma membrane of *Chara corallina* is electrically excitable. Depolarization of the membrane more positive than a critical threshold elicits a propagated action potential (AP) (Beilby and Coster, 1979). The bulk rise in membrane conductance, which underlies this transient membrane depolarization, is due to a short-lasting activation of Cl^- and K^+ channels (Homann and Thiel, 1994; Thiel et al., 1997). Because of the thermodynamic conditions, this leads to an efflux of KCl from the cytoplasm into the external medium (Kikuyama, 1986). Hence, the plant action potential is different from the AP in animal cells; it is osmotically active. This osmotic activity seems to be fundamental for the physiological role of the AP in *Chara* where it is apparently involved in the regulation of the internal pressure (turgor pressure) in the cell (Barry 1970; Shepherd et al., 2002).

The mechanism underlying the electrical stimulation of the AP is still not fully understood, but a rise in cytoplasmic Ca^{2+} undisputedly plays a key role (Williamson and Ashley, 1982; Kikuyama and Tazawa, 1983; Wacke and Thiel, 2001). This rise in Ca^{2+} is thought to activate Ca^{2+}-sensitive Cl^- channels (Okihara et al., 1991; Homann and Thiel, 1994)—the process that generates the depolarization. The activation of K^+ channels, which support repolarization, follows either as a result of the depolarization or in response to the rise in Ca^{2+} (Homann and Thiel, 1994; Thiel et al., 1997).

The classical view is that Ca^{2+} enters the cytoplasm via voltage-dependent channels (Tazawa and Kikuyama, 2003). Other investigations have revealed that the threshold for excitation is posed by a quasi all-or-none type liberation of Ca^{2+} from internal stores (Wacke and Thiel, 2001; Wacke et al., 2003). In this sense, the AP in *Chara* occurs not to function like a classical Hodgkin Huxley (HH) type AP. This means that the AP is not entirely based on the time- and voltage-dependent activation properties of plasma membrane ion channels but on a complex signal transduction cascade. Similar mechanisms of membrane excitation, which are based on Ca^{2+} release from internal stores, are also well known from animal cells where they are found in muscles (Nelson et al., 1995) and even some neurons (Chavis et al., 1996).

The latter type of a ''chemical'' action potential was in the past well-described by models, which include a nonlinear dynamic interplay of cytosolic Ca^{2+} ($[Ca^{2+}]_c$) and second messenger-stimulated release of Ca^{2+} from internal stores (Othmer, 1997). The same modeling approach was also

Submitted April 23, 2004, and accepted for publication October 13, 2004.

Address reprint requests to Zvonko Trontelj, Physics Department, University of Ljubljana, Jadranska 19, 1000 Ljubljana, Slovenia. Tel.: 386-1-476-6582; E-mail: zvonko.trontelj@fiz.uni-lj.si.

0006-3495/05/01/690/08 $2.00

doi: 10.1529/biophysj.104.044974

suitable to simulate a large spectrum of phenomena related to membrane excitation in *Chara* (Wacke et al., 2003). One parameter in this model, which is predicted to effect the kinetics of Ca^{2+} mobilization and hence the kinetics, is the cytoplasmic concentration of Ca^{2+} before stimulation.

To further prove the validity of the model, we therefore examine in this study the kinetics of the AP under conditions in which $[Ca^{2+}]_c$ is altered. This can be easily done by transferring the plants from the dark into the light, because it is known that $[Ca^{2+}]_c$ is in these cells reduced under the influence of light (Miller and Sanders, 1987; Plieth et al., 1998a).

This work also has a methodological aspect because the AP in *Chara* is examined with a noninvasive method by recording the magnetic field in the vicinity of a *C. corallina* internodal cell under different illumination conditions. According to Ampere's or the Biot-Savart law, measured magnetic field in the vicinity of intra- and extracellular currents carries information on these currents. Measurement of cellular magnetic field is also connected to the AP (Clark and Plonsey, 1966; Woosley et al., 1985) and can be thus a supplemental method to other electrophysiological investigations.

MATERIALS AND METHODS

C. corallina was cultured in the laboratory in a 90-liter aquarium (~60 cm high) filled with artificial pond water (APW) (0.1 mM KCl, 0.5 mM $CaCl_2$, 1 mM NaCl). The plants were grown on a layer of lake mud. A single internodal cell was prepared a day or two before the experiments and placed in APW + 2 HEPES, pH = 6.8–7.0 (NaOH). All salts were from Sigma Chemical (St. Louis, MO).

The internodal cell was held in a horizontal Plexiglas half-tube, similar to that previously described (Trontelj et al., 1994) and is schematically shown in Fig. 1 (*side view*) and Fig. 2 *A* (*top view*) . The leveling stage allowed the bath to be moved up and down to adjust the distance between the cell and the tail of the superconducting quantum interference device (SQUID) microscope Dewar vessel. A 10 μm thick Mylar film prevented contact between the cell and the SQUID microscope sapphire window and stabilized the position of the internodal *C. corallina* cell during scanning. One end of the internodal cell was mounted in a small Plexiglas compartment so as to electrically isolate this end of the cell (the *left end* in Fig. 1) from the bath with a petroleum jelly seal (Fig. 1). The Plexiglas compartment was filled with 100 mM KCl that served as a reference electrode (the K+ anesthesia technique) for parallel electrical measurements of the AP (Trontelj et al., 1994). We had to apply this technique so as not to disturb the SQUID sensor with ferromagnetic impurities of microelectrodes and the cell manipulating device. The Plexiglas half-tube with the internodal *C. corallina* cell and the 100 mM KCl compartment was submerged in a shallow Plexiglas container with the dimensions $20 \times 14 \times 4$ cm^3 (Fig. 1). Using Ag/AgCl electrodes, we measured the resting potential as the potential difference between the APW and the KCl compartment before stimulation. Before the measurements, both recording electrodes were immersed in the KCl compartment to cancel the junction and offset potential. We needed *C. corallina* internodal cells that were at least 8 cm long to allow simultaneous measurement of the electric potential differences (AP) and the associated magnetic field due to action currents (AC). For the measurements reported here, we selected internodal cells that were up to 15 cm long with diameters between 0.8 and 1.1 mm. The amplitude of the square wave electric stimulus with duration of 40–80 ms was adjusted above the threshold for the AP eliciting. The interstimulus interval was at least 120 s, and most cells were responsive to several tens of stimulations.

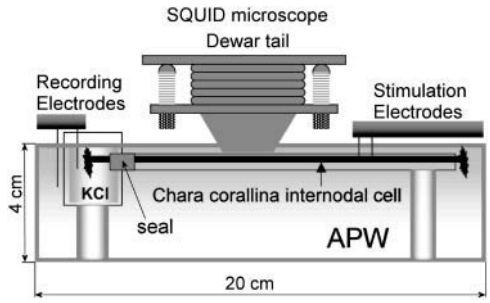

FIGURE 1 Schematic experimental setup (*side view*) used for electric and magnetic measurements on *Chara corallina* internodal cell. The Plexiglas holder supporting the cell is terminated on the left side in a sealed compartment to record the transmembrane potential.

The bath temperature was carefully monitored during each experiment and was maintained at 20.0°C. All measurements were performed in an air-conditioned, magnetically shielded room. During an average 2-h measuring session, the temperature varied by only 0.2°C.

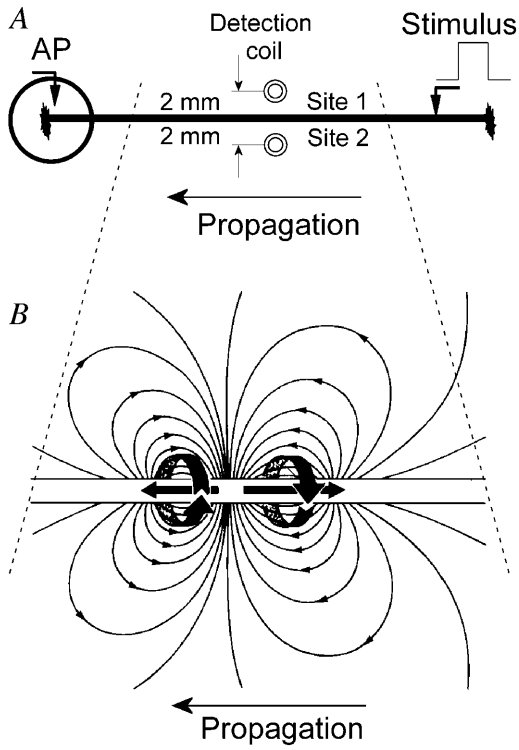

FIGURE 2 (*A*) Schematic of *Chara corallina* internodal cell (*top view*) indicating the location of the stimulus, the AP, and the magnetic field measurement sites. (*B*) Schematic distribution of intracellular current (two current dipoles within the internodal cell) and extracellular current (*thin lines*) for a propagating AP along the *Chara corallina* internodal cell. The contribution of the extracellular current to the measured magnetic field is negligible in an extended bath. The magnetic field due to the intracellular current in the vicinity of the internodal cell is represented as a ring around the cell. The depolarized part of the cell is shown on the left side, the repolarized on the right side.

The cell illumination was provided by a light source with a spectrum similar to daylight with 5–10 Wm^{-2} delivered to the cell by a fiber-optic bundle that passed through an opening into the magnetically shielded room to eliminate power supply noise of the light source.

By measuring magnetic fields in the vicinity of a *C. corallina* internodal cell after the AP was electrically elicited, we basically measure the contribution of total ionic current, associated with the propagating AP. The measured internodal *C. corallina* cell is in APW bath, and extracellular ionic currents, caused by the AP propagation along the cell, are spread through the whole APW volume. Their density is very small and their contribution to the measured magnetic field is negligible. Practically only the magnetic field due to axial intracellular current—we can call it the action current—can be measured. Taking the maximal intracellular current 1 μA and the distance from the cell geometrical axis 2 mm, we obtain by applying Ampere's law for the maximal value of magnetic field 10^{-10} T = 100 pT. To measure this magnetic field or even smaller magnetic fields, a very sensitive magnetic field sensor is needed. We can choose between a SQUID magnetometer (Drung, 1995), covering an area of several 100 cm^2 and a single SQUID magnetometer with a small detection coil (usually called a pickup coil) in a configuration that comes extremely close to the measured object—SQUID microscope (Baudenbacher et al., 2002). The second alternative enables us to obtain a high signal/noise ratio (small distance from the detection coil to the cell) and high spatial resolution (due to the small diameter of detection coil).

In our SQUID microscope design, a hand-wound niobium detection coil is coupled to a commercially available low temperature SQUID sensor. The SQUID sensor and the detection coil are in the vacuum space of the cryostat separated typically by ~100 μm from the room-temperature sample by a thin sapphire window. A computerized nonmagnetic scanning stage with submicron resolution in combination with a tripod leveling system allows samples to be scanned at levels of 10 μm below the sapphire window. For a 20-turn 500 μm diameter detection coil, we achieve a field sensitivity of 350 $fT/Hz^{-1/2}$ and for a 40-turn 1 mm diameter coil, 50 $fT/Hz^{-1/2}$ for frequencies above 1 Hz for the vertical component of the magnetic field. The voltage output of the SQUID electronics corresponding to the vertical magnetic field component generated by propagating AC was recorded at a bandwidth of DC-500 Hz for a period of 30 s at a position along the cell where the magnetic signal was maximal. The SQUID microscope, the sample, and the scanning stage were housed in a three layer, μ-metal magnetically shielded room (Vacuumschmelze, Hanau, Germany) to eliminate the influence of near-DC and higher frequency noise sources.

RESULTS

Measurements

Before the first measurement, the optimal position of the SQUID microscope detection coil has been determined. The coil was positioned 1–2 mm lateral and ~200 μm above the *C. corallina* internodal cell (Fig. 2 *A*) where the vertical component of the magnetic field was readily detectable (at least several 10 pT at maximum). The sapphire window of the SQUID microscope was positioned ~100 μm above the cell surface, resulting in a distance between the detection coil and the cell surface of ~200 μm. The signal/noise ratio was 5:1 or better for a single scan. A high temporal density of measurement points allowed us to improve the signal/noise ratio by averaging. We regularly confirmed that the signal reversed polarity (as expected for this geometry) after the scan crossed the geometrical axis of the cell.

Keeping the SQUID magnetometer's detection coil in position, denoted as ''Site 1'' in Fig. 2 *A*, we measured the magnetic field as a function of time. The result is shown in Fig. 3 *A*. Moving the bath with the *C. corallina* internodal cell so that the detection coil reaches position ''Site 2'' in Fig. 2 *A* causes the signal polarity to change (Fig. 3 *B*). Small differences in peak amplitudes between Fig. 3 *A* and *B* reflect scattering between two measuring sessions; a small deviation from symmetrically located measuring points possibly contributes to these differences as well.

The AP was measured simultaneously at a point along the cell 50 mm away from the detection coil position and is shown in Fig. 3 *C*. The separation of magnetic and electric measuring points leads to a time shift of 1.1–1.2 s. From these values, the AP propagation velocity can be calculated to be ~4 cm/s, which is in good agreement with the previous results (Trontelj et al., 1994). Before and during these measurements, the *C. corallina* internodal cell was kept in darkness for at least 1 h. The detection coil was placed 2 mm (Fig. 3 *B*) and –2 mm (Fig. 3 *A*) lateral to the internodal cell surface. The vertical distance from the detection coil to the cell surface was 200 μm. The measurements shown in Fig. 3 are a single-shot measurement with no averaging of the data.

The dotted line in Fig. 2 *A* denotes a small part of the internodal cell, which we assume is sufficiently long to cover both the repolarized and the depolarized area in this part of the internodal cell. The corresponding AC is in the form of two current dipoles (called also axial current elements) and is

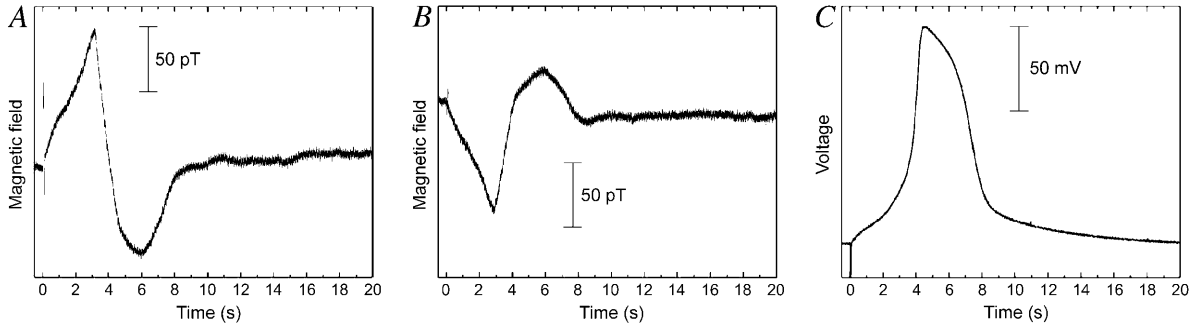

FIGURE 3 (*A*) Magnetic field measured at Site 2 as indicated in Fig. 2 *A*. (*B*) As in Fig. 3 *A* but at Site 1 indicated in Fig. 2 *A*. (*C*) AP recorded by the K+ anesthesia technique.

drawn as two thick arrows within the cell (Fig. 2 *B*). The left one belongs to the depolarized part and the right one to the repolarized part of the cell. The magnetic field around each current element is for clarity shown as one broad line in the ring form around the current element according to Ampere's law. Both magnetic fields have different directions since the current elements are pointing in opposite directions. Considering the constant AP propagation velocity c of 4 cm/s and the duration of depolarization 1 s, we get for the depolarized part of the cell $x = ct = 4$ cm. This means that for measurements very close to the *C. corallina* internodal cell, we have a similar situation as in the case of observing the magnetic field of a straight wire that is conducting electric current.

The relation between AP and AC (and corresponding magnetic field) in different nerve cells (Barach et al., 1980; Woosley et al., 1985; Trahms et al., 1989) and also in an excited single internodal cell of *C. corallina* (Slibar et al., 2000; Trontelj et al., 1994) was studied in detail. Briefly, in all studied cases, we observe that the peak forward action current occurs approximately simultaneously with the maximum time derivative of the AP, and the maximum backward action current occurs at the most rapid change in the AP during repolarization. The time of the peak AP corresponds to the zero-crossing between the forward and backward phases of the AC. The correlation of these AP and AC features are more pronounced in our measurements in this study since the small SQUID microscope detection coil can be placed closer to the cell. Fig. 3 illustrates these relations. However, we have to take into account in this particular case that AP and magnetic field were not measured at the same point along the cell (there is ~1.1 s time difference between both signals).

Under constant illumination and temperature, the transmembrane potential and the magnetic field generated by AC revealed only small variations either when different cells or when one *C. corallina* internodal cell was measured repetitively.

Fig. 4, traces *a–i*, show the time dependence of the vertical component of magnetic field measured at $y = 2$ mm lateral to the cell's geometrical axis under different illumination conditions. In this series of experiments, the internodal cell was in darkness for 60 min before the first measurement of AP propagation. Fig. 4, trace *a*, shows the magnetic field generated by AC just before the light was turned on. Subsequent recordings were done under constant illumination after particular time intervals as shown in Fig. 4, traces *b–e*. It can be seen that, as a response to illumination, the temporal evolution of the magnetic field changes over a period of <1 h before reaching a new steady state. Most pronounced is the time shift of the positive peak of the magnetic signal associated with the depolarization. The negative peak associated with the repolarization is less expressed.

The temporal characteristic of the magnetic field is reversible. Upon transferring the cell back from light into darkness, the temporal field changes became progressively closer to the initially measured magnetic field as shown in the sequence Fig. 4, traces *f–i*.

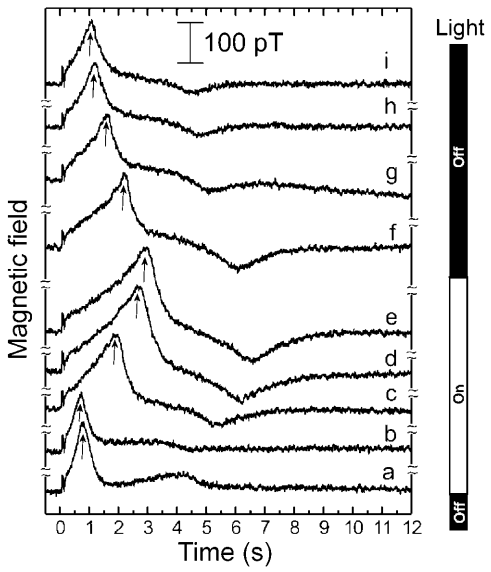

FIGURE 4 Recordings of the time-dependent vertical component of the magnetic field generated by a propagating AC measured as a function of illumination starting after 1 h dark accommodation. Trace *a*, light off; trace *b*, 10 min light on; trace *c*, 20 min light on; trace *d*, 30 min light on; trace *e*, 40 min light on (here we waited for an additional 20 min to complete 1 h in the light accommodation); trace *f*, 10 min light off; trace *g*, 20 min light off; trace *h*, 30 min light off; and trace *i*, 40 min light off. Small arrows indicate where the temporal shift was observed.

Parallel electrical measurements (Fig. 5, traces *b–e* and *f–i*) demonstrate a similar dependence of the AP time evolution on light/darkness. A transition of a cell from darkness to light prolonged the duration of the membrane depolarization for ~2 s after a transitional period of ~20–30 min on average. The depolarization time prolongation was accompanied by an increase in the depolarization peak of ~10–15%. This can be attributed to the hyperpolarization of the resting potential under illumination (Mimura and Tazawa, 1986).

The time shifts extracted from the magnetic measurements from eight cells are shown in Fig. 6. To better compare different cells, we introduced a normalization as a dimensionless quantity, $\alpha = \Delta t/t_o$. Here, Δt is the light-induced delay with respect to the initial AC measured as the temporal shift in the depolarization maximum and t_o the time of the depolarization maximum for a particular illumination/darkness condition relative to the stimulus. We see that α increases with the duration of illumination when cells are transferred from darkness into constant light. Fig. 7 summarizes the dependence of the average value of the normalized time delay α as a function of illumination time obtained from AP measurements on 15 *C. corallina* internodal cells. Figs. 6 and 7 demonstrate the behavior of α obtained from magnetic field (AC) and AP measurements of cells exposed to different

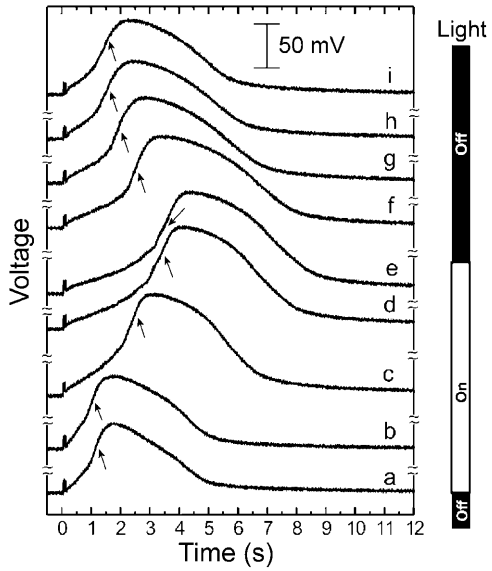

FIGURE 5 Recordings of the time dependence of the AP measured as a function of illumination simultaneous with magnetic measurements starting after 1 h dark accommodation. Trace *a*, light off; trace *b*, 10 min light on; trace *c*, 20 min light on; trace *d*, 30 min light on; trace *e*, 40 min light on (here we waited for an additional 20 min to complete 1 h in the light accommodation); trace *f*, 10 min light off; trace *g*, 20 min light off; trace *h*, 30 min light off; and trace *i*, 40 min light off. Small arrows indicate the points, corresponding to those that were observed in Fig. 4.

durations of illumination. Both curves are almost identical. In addition, we also see that error bars in Fig. 7 are shorter (here were considered more cells).

The reversible effect of light/dark transitions on the kinetics of membrane excitation suggests a coupling between photosynthesis and membrane excitation. To examine this hypothesis, we have measured the influence of a common photosynthesis inhibitor, DCMU (3,-(3,4-dichlorophenyl)-1, 1-dimethylurea), at a concentration of 10 μM on the kinetics

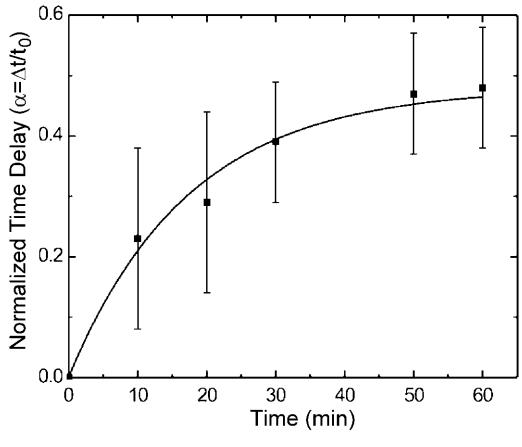

FIGURE 6 Averaged normalized temporal shift of the maximum of the measured magnetic field (AC) with increasing illumination exposure time. Eight cells were considered.

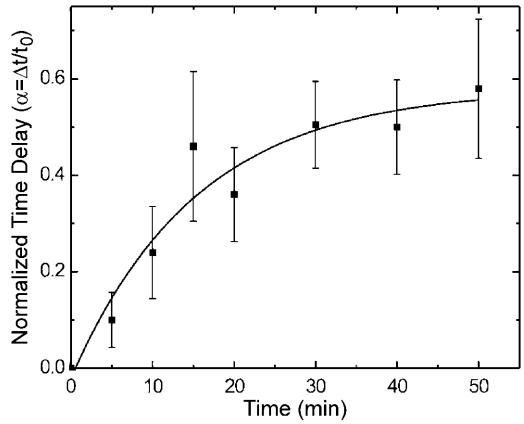

FIGURE 7 Averaged normalized temporal shift of the maximum of the measured AP with increasing illumination exposure time. Fifteen cells were considered.

of excitation. In this case, a *C. corallina* cell was exposed to light for a period of 60 min in the presence of DCMU in the bath solution. After ~20 min, the magnetic signal intensity started to decrease in a way reminiscent of the behavior in the dark, as expected from our data in the illumination studies. Two cells were tested with both showing the same behavior.

Modeling

C. corallina internodal cells are, to a very good approximation, cylindrically symmetric and therefore ideally suitable for electrophysiological model studies. Several models followed the HH work on the nerve axon (Hodgkin and Huxley, 1952) and were adapted to *C. corallina* internodal cells (Beilby, 1982) or were devoted to studies of relations between AP, AC, and associated magnetic field (Clark and Plonsey, 1966; Woosley et al., 1985; Slibar et al., 2000). Here we will try to show that AP in *C. corallina* internodal cells experiences similarity to AP in those animal cells (heart, brain) where the ''biochemical AP'' is known to exist in addition to HH AP.

The HH type model is based purely on the kinetics of plasma membrane channels and the electrical properties of membrane but does not account for changes in $[Ca^{2+}]_c$. This factor, however, requires consideration in the context of this study because alterations in $[Ca^{2+}]_c$ were observed experimentally under the influence of light/dark transitions (Miller and Sanders, 1987) and are in qualitative agreement with our model prediction. We have used an extended model of Othmer (Wacke et al., 2003), which describes the dynamics of $[Ca^{2+}]_c$ in the context of a second messenger system. In that model, the AP in *Chara* is successfully described by an electrically stimulated release of Ca^{2+} from internal stores. The resulting changes in membrane conductance are the direct consequence of this dynamic change in $[Ca^{2+}]_c$. In this extended model, the thresholdlike dependence of Ca^{2+}

mobilization on electrical stimulation can be simulated by combining the following two processes:

i. The voltage-dependent synthesis/breakdown of the second messenger inositol 1,4,5-trisphosphate (IP_3).
ii. The concerted action of IP_3 and Ca^{2+} on the gating of the receptor channels, which conduct Ca^{2+} release from internal stores.

The model has been proved suitable to simulate a range of experimental results in the context of the AP in *Chara*, including a complex behavior of Ca^{2+} mobilization under periodic stimulation with higher-order phase locking and irregular responses upon increased stimulation frequency. This demonstrates that the all-or-none type activation of the action potential is only the consequence of the preceding all-or-none type mobilization of Ca^{2+} from internal stores. The dependency of the gating of the receptor channel on $[Ca^{2+}]_c$ suggests that the Ca^{2+} concentration before stimulation of the AP has an influence on the following excitation kinetics.

To examine the effect of variable $[Ca^{2+}]_c$ on the kinetics of the electrically stimulated changes in Ca^{2+}, we modified the model as follows: Cells move excess Ca^{2+} from the cytoplasm back into internal stores by an endogenous Ca^{2+} pump system (e.g., Reddy, 2001). In the model, this process is accounted for by a Hill function:

$$\bar{g}(C) = \frac{\bar{p}_1 C^4}{C^4 + \bar{p}_2^4}. \quad (1)$$

In this equation, $\bar{p}_1$ and $\bar{p}_2$ are the Hill coefficients, and C is the cytosolic Ca^{2+} concentration. For more details, see Othmer (1997). To achieve different $[Ca^{2+}]_c$ under resting conditions, which are known to occur during light/dark transitions (Miller and Sanders, 1987; Plieth et al., 1998a), we varied the Hill factor $\bar{p}_2$ in Eq. 1. This procedure is only an indirect approach, since the chloroplasts from which the Ca^{2+} originates during light/dark transitions (Miller and Sanders, 1987) are not considered as extra Ca^{2+} pool in the model for $[Ca^{2+}]_c$ dynamics. Nonetheless, this simple manipulation of the model should be sufficient to provide basic insight into the dependency of Ca^{2+} mobilization on $[Ca^{2+}]_c$.

Fig. 8 illustrates the results of this simulation. As a consequence of reduced Ca^{2+} pump activity, the resting $[Ca^{2+}]_c$ increases over the physiological range from ~20 nM to 200 nM. This roughly covers the changes in $[Ca^{2+}]_c$ of 50–250 nM found in response to light/dark transitions in *Chara* (Miller and Sanders, 1987; Plieth et al., 1998a). The simulation further shows that an elevation of $[Ca^{2+}]_c$ before the stimulation results in a progressive shortening of the delay time between stimulation and the rapid phase of $[Ca^{2+}]_c$ rise. The dependence of this delay time on the resting $[Ca^{2+}]_c$ concentration is plotted in the inset of Fig. 8.

On the assumption that the change in membrane voltage during the AP is only the consequence of an activation of

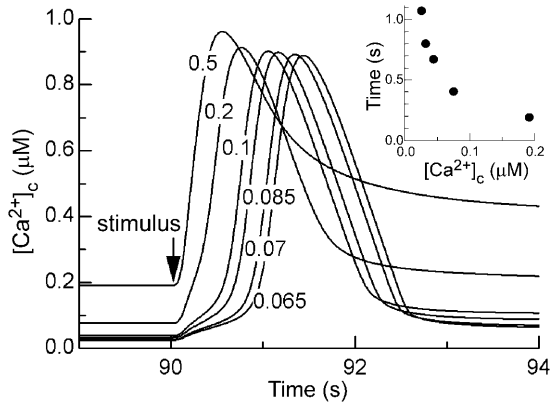

FIGURE 8 Simulated $[Ca^{2+}]_c$ transients in response to a single electrical stimulation (100 ms/5 μA). Data were calculated with model parameters reported in Wacke et al. (2003). Different curves are obtained by changing the Hill coefficients p_2 in the model term, which describes the buffering of $[Ca^{2+}]_c$. An increase in p_2 over a range of 0.065 μM–0.5 μM results in reduced Ca^{2+} buffering and a consequent increase in the resting $[Ca^{2+}]_c$. In the simulation, pulses were started after 90 s in which the system was allowed to equilibrate. (*Inset*) Delay time between stimulus and maximal slope of $[Ca^{2+}]_c$ increase as a function of resting $[Ca^{2+}]_c$ before stimulation.

$[Ca^{2+}]_c$-sensitive Cl^- channels (Biskup et al., 1999; Thiel et al., 1997), the model simulation compares well with the experimental data. The assumed progressive decrease in $[Ca^{2+}]_c$ of ~150 nM after the transition from dark to light results in an increasing delay time between the electrical stimulus and the rapid phase of $[Ca^{2+}]_c$ rise, or the activation of the Cl^- channels, respectively.

ANALYSIS AND DISCUSSION

The results of our measurements and subsequent model studies demonstrate the potential of using noninvasive magnetic measurements as a way to obtain information about the axial intracellular action currents associated with depolarization and repolarization of the membrane potential during AP propagation (Woosley et al., 1985). This current reflects the summed contribution of all transmembrane ionic currents as well as electrogenic transport and other secondary transport processes in intracellular compartments. The SQUID microscope with its high spatial resolution will be a convenient instrument in studying these events in details. In those cases where different transmembrane ionic currents can be observed as transiently separable events, the analysis and the interpretation of the data can be undertaken. This is possible, for example, in the case of the influence of light on the kinetics of ionic currents during the AP.

The main observation in this work was that a transfer of cells from the light into the dark resulted in an appreciable and reversible change in the kinetics of the action potential. Predominantly, the first part of the AC/AP temporal evolution, i.e., the slow depolarization part, increased progressively with time of light exposure; the rapid part of the AP,

including depolarization and repolarization, was on the other hand only marginally affected. These observed changes in the kinetics of the *Chara* AP could in principle be modeled by a classical HH approach by adding a variable delay factor. However, there is no mechanistic motivation for such a delay factor, and it is difficult to envisage how a first-order voltage-dependent process could produce such a long and variable delay.

The experimental observations are, on the other hand, fully consistent with the view that the AP in *Chara* is of a ''chemical'' nature, i.e., based on a quasi all-or-none type liberation of Ca^{2+} from internal stores (Wacke and Thiel, 2001; Wacke et al., 2003). The model for the *Chara* AP (Wacke et al., 2003) predicts that a decrease of the resting $[Ca^{2+}]_c$ by ~250 nM, as is expected to occur in response to a dark/light transition (Miller and Sanders, 1987; Plieth, 1995), causes a delay in the onset of the rapid rise in $[Ca^{2+}]_c$ during excitation. Assuming that the activation of the Cl^- channels, which cause the depolarization, is the direct consequence of the change in $[Ca^{2+}]_c$, the measured data nicely match the model prediction, even on a quantitative basis. The model further predicts that a modulation of the resting $[Ca^{2+}]_c$ has no big effect on the kinetics of the bulk changes of $[Ca^{2+}]_c$. Again, this prediction is met by the present data because the features in the temporal evolution of the AC/AP were basically unchanged.

Previous measurements have assessed the changes in $[Ca^{2+}]_c$ after light/dark transitions indirectly by recording the velocity of cytoplasmic streaming, because this velocity is proportional to $[Ca^{2+}]_c$ (Mccurdy and Harmon, 1992). In long-term recordings, Plieth and co-workers (Plieth et al., 1998b) found that it took ~30 min to achieve a steady streaming velocity after transferring plants from dark to light. A slow time course for the change in Ca^{2+} in a similar order of magnitude can also be deduced from direct recordings of $[Ca^{2+}]_c$ in *Chara*. The usual rise in $[Ca^{2+}]_c$ after light/dark transitions was even after 5 min in the dark not yet fully saturated (Plieth, 1995). Hence, the time course in Ca^{2+} changes after light/dark transitions are of the same order of magnitude as the one we found in our measurements within experimental errors. Therefore, the entire observation of the change in the AP kinetics found under light/dark transition can be quantitatively explained by a slow progressing change in the resting $[Ca^{2+}]_c$ and a consequent modulation of this parameter on the release of Ca^{2+} from internal stores.

CONCLUSION

We performed electric measurements of the AP in parallel with noninvasive magnetic measurements of the associated action current and found an excellent correspondence. The temporal evolution of electric and magnetic signals and the modeling study enabled us to associate the altered depolarization of illuminated *Chara corallina* internodal cells with changes in the cytoplasmic concentration of Ca^{2+} ions in combination with a second messenger cascade. This is consistent with the view of a biochemical nature of electrically elicited AP and AC in these cells.

Our experimental results demonstrate the potential of SQUID microscope imaging for noninvasive magnetic measurements of axial intracellular current in electrically stimulated single internodal cells of *Chara corallina* under the influence of light. This kind of measurement provides a valuable technique to complement the longer existing electrophysiological methods in studies of plant cells.

Our sincere thanks to Dr. Randy Wayne of Cornell University for providing us with specimens of *Chara corallina* algae. We thank John Wikswo for his hospitality (Z.T.) and comments on this manuscript. One of us (L.F.) would like to thank to Mary J. Beilby for the program information on the calculation of temporal evolution of AP in *Chara corallina*.

This research has been supported in part by a National Research Council Collaboration in Basic Science and Engineering program and by National Institutes of Health (NIH) grants R42 GM54963 and R01 HL58241. The SQUID microscope has been developed under NIH grant R42GM54963 and National Science Foundation grant DBI 9604948.

REFERENCES

Barach, J. P., J. A. Freeman, and J. P. Wikswo Jr. 1980. Experiments on the magnetic field of nerve action potentials. *J. Appl. Phys.* 51:4532–4538.

Barry, P. H. 1970. Volume flows and pressure changes during an action potential in cells of *Chara australis*. I. Experimental results. *J. Membr. Biol.* 3:313–334.

Baudenbacher, F., N. T. Peters, and J. P. Wikswo. 2002. High resolution low-temperature superconductivity superconducting quantum interference device microscope for imaging magnetic fields of samples at room temperatures. *Rev. Sci. Instrum.* 73:1247–1254.

Beilby, M. J. 1982. Cl^- channels in *Chara*. *Philos. Trans. R. Soc. Lond. B Biol. Sci.* 299:435–445.

Beilby, M. J. 1990. Current-voltage curves for plant membranes: a critical analysis of the method. *J. Exp. Bot.* 41:165–182.

Beilby, M. J., and H. G. L. Coster. 1979. The action potential in *Chara corallina*. II. Two activation-inactivation transients in voltage clamps of the plasmalemma. *Aust. J. Plant Physiol.* 6:323–335.

Biskup, B., D. Gradmann, and G. Thiel. 1999. Calcium release from $InsP_3$-sensitive internal stores initiates action potential in *Chara*. *FEBS Lett.* 453:72–76.

Chavis, P., L. Fagni, J. B. Lansman, and J. Bockaert. 1996. Functional coupling between ryanodine receptors and L-type calcium channels in neurons. *Nature.* 382:719–722.

Clark, J. W., and R. Plonsey. 1966. A mathematical evaluation of the core conductor model. *Biophys. J.* 6:95–112.

Drung, D. 1995. The PTB 83-SQUID system for biomagnetic applications in a clinic. *IEEE T. Appl. Supercon.* 5:2112–2117.

Hodgkin, A. L., and A. F. Huxley. 1952. A quantitative description of membrane current and its application to conductance and excitation in nerve. *J. Physiol. (Lond.).* 117:500–544.

Homann, U., and G. Thiel. 1994. Cl^- and K^+ channel currents during the action potential in *Chara*; simultaneous recording of membrane voltage and patch currents. *J. Membr. Biol.* 141:297–309.

Hope, A. B., and G. P. Findlay. 1964. The action potential in *Chara*. *Plant Cell Physiol.* 5:377–379.

Hope, A. B., and N. A. Walker. 1975. Physiology of Giant Algal Cells. Cambridge University Press, London.

Karol, K. G., R. M. McCourt, M. T. Cimino, and C. F. Delwiche. 2001. The closest living relatives of land plants. *Science.* 294:2351–2353.

Kikuyama, M. 1986. Ion efflux during excitation of Characeae. *Plant Cell Physiol.* 27:1213–1216.

Kikuyama, M., and M. Tazawa. 1983. Transient increase of intracellular Ca^{2+} during excitation of tonoplast-free *Chara* cells. *Protoplasma.* 117:62–67.

Kranz, H. D., D. Miks, M. L. Siegler, I. Capesius, C. W. Sense, and V. A. Huss. 1995. The origin of land plants: phylogenetic relationships among charophytes, bryophytes, and vascular plants inferred from complete small-subunit ribosomal RNA gene sequences. *J. Mol. Evol.* 4:74–84.

Mccurdy, D. W., and A. C. Harmon. 1992. Calcium-dependent protein-kinase in the green-alga *Chara*. *Planta.* 188:54–61.

Miller, A. J., and D. Sanders. 1987. Depletion of cytosolic free calcium induced by photosynthesis. *Nature.* 326:397–400.

Mimura, T., and M. Tazawa. 1986. Light-induced membrane hyperpolarization and adenin nucleotide levels in perfused Characean cells. *Plant Cell Physiol.* 27:319–330.

Nelson, M. T., H. Cheng, M. Rubart, L. F. Santana, A. D. Bonev, H. J. Knot, and W. J. Lederer. 1995. Relaxation of arterial smooth muscle by calcium sparks. *Science.* 270:633–637.

Okihara, K., T. Ohkawa, I. Tsutsui, and M. Kasai. 1991. A calcium dependent and voltage-dependent chloride-sensitive anion channel in the *Chara* plasmalemma. A patch clamp study. *Plant Cell Physiol.* 32:593–602.

Othmer, H. G. 1997. Signal transduction and second messenger systems. *In* Case Studies in Mathematical Modeling—Ecology, Physiology and Cell Biology. H. G. Othmer, F. R. Adler, M. A. Lewis, and J. Dallon, editors. Prentice Hall, Upper Saddle River, NJ. 99–126.

Plieth, C. 1995. Estimation of ion concentrations and their variations in cells and tissues of green plants using image analysis as ratiometric fluorescence microscopy and laser Doppler anemometry. PhD thesis. University of Kiel, Germany.

Plieth, C., B. Sattelmacher, and U. P. Hansen. 1998a. Light-induced cytosolic calcium transients in green plant cells. I. Methodological aspects of chlorotetracycline usage in algae and higher-plant cells. *Planta.* 207:42–51.

Plieth, C., B. Sattelmacher, and U. P. Hansen. 1998b. Light-induced cytosolic calcium transients in green plant cells. II. The effect on a K^+ channel as studied by a kinetic analysis in *Chara corallina*. *Planta.* 207:52–59.

Reddy, A. S. N. 2001. Calcium: silver bullet in signaling. *Plant Sci.* 160: 381–404.

Shepherd, V., M. Beilby, and T. Shimmen. 2002. Mechanosensory ion channels in charophyte cells: the response to touch and salinity stress. *Eur. Biophys. J.* 31:341–355.

Shimmen, T., T. Mimura, M. Kikuyama, and M. Tazawa. 1994. Characean cells as a tool for studying electrophysiological characteristics of plant cells. *Cell Struct. Funct.* 19:263–278.

Slibar, M., Z. Trontelj, V. Jazbinsek, G. Thiel, and W. Mueller. 2000. Magnetic field and electric potential of excited plant cell *Chara corallina*: calculation and comparison with experiment. *In* Biomag 96: Proceedings of the Tenth International Conference on Biomagnetism. C. J. Aine, Y. Okada, G. Stroink, S. J. Swithenby, and C. C. Wood, editors. Springer, New York. 679–682.

Tazawa, M., and M. Kikuyama. 2003. Is Ca^{2+} release from internal stores involved in membrane excitation in Characean cells? *Plant Cell Physiol.* 44:518–526.

Tazawa, M., T. Shimmen, and T. Mimura. 1987. Membrane control in the Characeae. *Annu. Rev. Plant Physiol.* 38:95–117.

Thiel, G., U. Homann, and C. Plieth. 1997. Ion channel activity during the action potential in *Chara*: new insights with new techniques. *J. Exp. Bot.* 48:609–622.

Trahms, L., S. N. Erne, Z. Trontelj, G. Curio, and P. Aust. 1989. Biomagnetic functional localization of a peripheral nerve in man. *Biophys. J.* 55:1145–1153.

Trontelj, Z., R. Zorec, V. Jazbinsek, and S. N. Erné. 1994. Magnetic detection of a single action potential in *Chara corallina* internodal cells. *Biophys. J.* 66:1694–1696.

Umrath, K. 1929. On the excitation propagation in higher plants. *Planta.* 7:174–207.

Wacke, M., G. Thiel, and M. T. Hütt. 2003. Ca^{2+} dynamics during membrane excitation of green alga *Chara*: model simulations and experimental data. *J. Membr. Biol.* 191:179–192.

Wacke, M., and G. Thiel. 2001. Electrically triggered all-or-none Ca^{2+} liberation during action potential in the giant alga *Chara*. *J. Gen. Physiol.* 118:11–21.

Williamson, R. E., and C. C. Ashley. 1982. Free Ca^{2+} and cytoplasmic streaming in the alga *Chara*. *Nature.* 296:647–651.

Woosley, J. K., B. J. Roth, and J. P. Wikswo Jr. 1985. The magnetic field of a single axon: a volume conductor model. *Math. Biosci.* 76:1–36.